Computer Physics Communications 192 (2015) 114–123

Contents lists available at ScienceDirect

Computer Physics Communications

journal homepage: www.elsevier.com/locate/cpc

Improved analytical representation of combinations of Fermi–Dirac integrals for finite-temperature density functional calculations

Valentin V. Karasiev *, Debajit Chakraborty, S.B. Trickey

Quantum Theory Project, Departments of Physics and of Chemistry, University of Florida, Gainesville FL 32611-8435, United States

ARTICLE INFO

Article history:
Received 6 November 2014
Received in revised form
27 February 2015
Accepted 2 March 2015
Available online 9 March 2015

Keywords:
Finite-temperature DFT
Non-interacting orbital-free free-energy
Exchange free-energy
Gradient expansion

ABSTRACT

Smooth, highly accurate analytical representations of Fermi–Dirac (FD) integral combinations important in free-energy density functional calculations are presented. Specific forms include those that occur in the local density approximation (LDA), generalized gradient approximation (GGA), and fourth-order gradient expansion of the non-interacting free energy as well as in the LDA and second-order gradient expansion for exchange. By construction, all the representations and their derivatives of any order are continuous on the full domains of their independent variables. The same type of technique provides an analytical representation of the function inverse to the FD integral of order 1/2. It plays an important role in physical problems related to the electron gas at finite temperature. From direct evaluation, the quality of these improved representations is shown to be substantially superior to existing ones, many of which were developed before the era of large-scale computation or early in the era.

1. Introduction

Finite-temperature density functional theory (DFT), whether in orbital-free (OF) or conventional Kohn–Sham (KS) form [1–3], has emerged as a major theoretical and computational tool for warm dense matter (WDM) studies [4–6]. In the OFDFT setting, non-interacting free-energy functionals in the local density approximation (LDA) [7], gradient-corrected [8,9], and generalized gradient approximation (GGA) [10] forms all involve various combinations of Fermi–Dirac (FD) integrals. In both OFDFT and KS form, exchange–correlation (XC) functionals with explicit temperature (T) dependence are important for accurate treatment of the WDM regime [11]. The finite-temperature LDA exchange energy functional and corresponding gradient correction also are expressed as combinations of FD integrals [12–16].

Fast, reliable implementation of all these functionals in DFT codes requires accurate analytical representations of those intrinsic FD integral combinations and their derivatives of low order. Our experience [10] is that the available representations are not always adequate for present-day requirements. An illustrative difficulty is with the often-cited representation in Ref. [8]. Details are below. A motivating issue is that the representation is on two sub-domains of the independent variable. As a result, the second derivative may behave badly in the vicinity of the joining of those two pieces. A second issue is that some of the available representations were developed before the era of digital computing or early in it, so that the precision of such fits (and of the constants in them) is coarse by modern standards.

Here we present accurate analytical representations for FD integral combinations that occur frequently in finite-T DFT and are important, therefore, for computation. The representations are in the form of Padé approximants [17] or Padé approximants modified by additional logarithmic terms. Some of the parameters for each quantity are constrained to match the zero-T and high-T series expansions for that quantity, with the remaining parameters determined by fits to accurately evaluated reference data. The techniques are similar to those used recently for accurate parametrization of the XC energy of the homogeneous electron gas (HEG) at finite T [11]. Comparison with some existing fits for the same quantities shows that our procedures yield much better accuracy.

The presentation is organized as follows. Section 2 summarizes FD integral combinations important in finite-T DFT. Section 3 delineates asymptotic constraints that are crucial to well-behaved analytical representations of those combinations. Section 4 considers the inverse function most relevant to finite-T DFT, and its asymptotic expansions. Section 5 describes the analytical representations and accuracy tests of them. Parameters of all the analytical forms are tabulated in the Appendix. Hartree atomic units are used throughout.

* Corresponding author.
E-mail address: vkarasev@ufl.edu (V.V. Karasiev).

http://dx.doi.org/10.1016/j.cpc.2015.03.002
0010-4655/

2. Important Fermi–Dirac integral combinations in finite-T DFT

A key quantity in finite-T OFDFT is the non-interacting free-energy density of the homogeneous electron gas of density n. It is given by the Thomas–Fermi combination of FD integrals [7]

$$f_s^{\rm TF}(n,{\rm T}) = \frac{\sqrt{2}}{\pi^2\beta^{5/2}}\Big[-\frac{2}{3}I_{3/2}(\eta)+\eta I_{1/2}(\eta)\Big], \tag{1}$$

where $\eta := \beta\mu$, $\beta := (k_{\rm B}{\rm T})^{-1}$. I_α is the FD integral [9]

$$I_\alpha(\eta) := \int_0^\infty dx \frac{x^\alpha}{1+\exp(x-\eta)}, \quad \alpha > -1$$

$$I_{\alpha-1}(\eta) = \frac{1}{\alpha}\frac{d}{d\eta}I_\alpha(\eta), \quad \alpha \neq 0, \tag{2}$$

and μ is the chemical potential defined by the density n as

$$n = \frac{\sqrt{2}}{\pi^2\beta^{3/2}}I_{1/2}(\beta\mu). \tag{3}$$

Remark. There are at least two conventional definitions of FD integrals as well as variations. The definition used here [9,18] is related to the one used by Huang [19], denoted as $f_{3/2}(w) = (2/\sqrt{\pi})I_{1/2}(\ln w)$.

It is convenient to define the reduced temperature

$$t = {\rm T}/{\rm T_F} = \frac{2}{\beta[3\pi^2 n]^{2/3}} \tag{4}$$

in terms of which Eq. (3) becomes

$$I_{1/2}(\beta\mu) = \frac{2}{3t^{3/2}}. \tag{5}$$

Since $I_{1/2}(\eta)$ is a strictly increasing function of $\eta = \beta\mu$, it follows that all functions of η are functions of the reduced temperature t. Sometimes a related variable

$$y(\eta) := I_{1/2}(\eta) \equiv \frac{2}{3t^{3/2}} \tag{6}$$

is used instead of t.

Returning to Eq. (1), we have

$$f_s^{\rm TF}(n,{\rm T}) = \frac{n}{\beta}f(\eta) \equiv \tau_0^{\rm TF}(n)\kappa(\eta), \tag{7}$$

where $\tau_0^{\rm TF}(n) = (3/10)(3\pi^2)^{2/3}n^{5/3}$ and

$$f(\eta) := \frac{1}{I_{1/2}(\eta)}\Big[-\frac{2}{3}I_{3/2}(\eta)+\eta I_{1/2}(\eta)\Big], \tag{8}$$

$$\kappa(\eta) := \frac{5\times 2^{2/3}}{3^{5/3}}\frac{1}{I_{1/2}^{5/3}(\eta)}\Big[-\frac{2}{3}I_{3/2}(\eta)+\eta I_{1/2}(\eta)\Big]. \tag{9}$$

The functions f and κ have a simple relation

$$\kappa(\eta) = \frac{5}{3}tf(\eta). \tag{10}$$

These two comparatively simple functions, together with the inverse problem for Eq. (6) (to find $\eta(y)$), illustrate the issue addressed here. Computational performance demands accurate analytical representations of such quantities. Achieving such representations for κ or f as a function of η or $y(\eta)$ requires development of suitably constrained analytical forms and fitting of them to accurately calculated reference values. An example is the work of Perrot, who used the variable y and provided an analytical fit for $f(y)$ on two y intervals [8]. Use of two intervals is an issue noted already and considered further below.

Another important category of FD integral combinations arises from density-gradient contributions. The finite-T generalized gradient approximation (GGA) [10] for the non-interacting free-energy uses T-dependent variables defined by analysis of the second-order gradient expansion (SGE) of the non-interacting free energy density of the weakly inhomogeneous electron gas [8,20]. The gradient term in the SGE has the coefficient

$$f_s^{(2)}(n,\nabla n,{\rm T}) = \tau_0^{\rm TF}(n)\frac{5}{27}s^2\widetilde{B}, \tag{11}$$

where $s = |\nabla n|/2(3\pi^2)^{1/3}n^{4/3}$, along with the definition

$$\widetilde{B}(\eta) := -3\frac{I_{1/2}(\eta)I_{-3/2}(\eta)}{I_{-1/2}^2(\eta)}. \tag{12}$$

High-quality representation of $\widetilde{B}$ thus is required.

Remark. the quantity $\widetilde{B}$ defined here is $\tilde{h}$ in the notation of Ref. [10].

The fourth-order term in the gradient expansion for the non-interacting free energy density derived in Refs. [20,21,9] takes the form

$$f_s^{(4)}(n,\nabla n,\nabla^2 n,{\rm T}) = \tau_0^{\rm TF}(n)\Big[\frac{8}{81}p^2\widetilde{C}-\frac{1}{9}s^2p\widetilde{D}+\frac{8}{243}s^4\widetilde{E}\Big], \tag{13}$$

where $p := \nabla^2 n/4(3\pi^2)^{2/3}n^{5/3}$. The ingredient combinations of FD integrals are

$$\widetilde{C}(\eta) := \frac{5\times 3^{11/3}}{2^{11/3}}I_{1/2}^{5/3}(\eta)\Big[\frac{1}{9}\frac{I_{-3/2}^2(\eta)}{I_{-1/2}^3(\eta)}-\frac{1}{5}\frac{I_{-5/2}(\eta)}{I_{-1/2}^2(\eta)}\Big], \tag{14}$$

$$\widetilde{D}(\eta) := \frac{5\times 2^{1/3}}{3^{1/3}}I_{1/2}^{8/3}(\eta)\Big[-3\frac{I_{-7/2}(\eta)}{I_{-1/2}^3(\eta)} + \frac{33}{10}\frac{I_{-3/2}(\eta)I_{-5/2}(\eta)}{I_{-1/2}^4(\eta)}-\frac{I_{-3/2}^3(\eta)}{I_{-1/2}^5(\eta)}\Big], \tag{15}$$

and

$$\widetilde{E}(\eta) := \frac{5\times 3^{14/3}}{2^{2/3}}I_{1/2}^{11/3}(\eta)\Big[-\frac{7}{96}\frac{I_{-9/2}(\eta)}{I_{-1/2}^4(\eta)} - \frac{1}{15}\frac{I_{-3/2}^2(\eta)I_{-5/2}(\eta)}{I_{-1/2}^6(\eta)}+\frac{1}{72}\frac{I_{-3/2}^4(\eta)}{I_{-1/2}^7(\eta)} + \frac{1}{12}\frac{I_{-3/2}(\eta)I_{-7/2}(\eta)}{I_{-1/2}^5(\eta)}+\frac{1}{32}\frac{I_{-5/2}^2(\eta)}{I_{-1/2}^5(\eta)}\Big]. \tag{16}$$

Exchange and correlation also are expressed in terms of FD integral combinations. For the weakly inhomogeneous electron gas at finite T, the LDA exchange (X) free-energy density [8,12] is

$$f_{\rm x}^{\rm LDA}(n,{\rm T}) = -\frac{1}{2\pi^3\beta^2}\int_{-\infty}^{\eta}[I_{-1/2}(\eta)]^2 d\eta, \tag{17}$$

or

$$f_{\rm x}^{\rm LDA}(n,{\rm T}) = \widetilde{A}_{\rm x}(n,{\rm T})e_{\rm x}^{\rm LDA}(n). \tag{18}$$

Here $e_{\rm x}^{\rm LDA}(n) = -\frac{3}{4}\Big(\frac{3}{\pi}\Big)^{1/3}n^{4/3}$ is the zero-T LDA X energy density (evaluated, of course, with the finite-T density) and the relevant FD

Table 1
Cross-reference of equation numbers for quantities considered in the present work and the corresponding analytical forms for fits and for Tables of coefficients for those fits.

Quantity	Definition	Analytical form	Coefficient values
$\widetilde{B}$	Eq. (12)	Eq. (37)	Table 3
$\widetilde{C}$	Eq. (14)	Eq. (38)	Table 4
$\widetilde{D}$	Eq. (15)	Eq. (38)	Table 5
$\widetilde{E}$	Eq. (16)	Eq. (38)	Table 6
$\widetilde{A}_{\rm x}$	Eq. (19)	Eq. (39)	Table 7
$\widetilde{B}_{\rm x}$	Eq. (21)	Eq. (40)	Table 8
$\eta_{1/2}$	Eq. (32)	Eq. (41)	Table 9

integral combination is

$$\widetilde{A}_{\rm x}(\eta) := \frac{f_{\rm x}^{\rm LDA}(n,{\rm T})}{e_{\rm x}^{\rm LDA}(n)} = \frac{2^{1/3}}{3^{4/3}}\frac{\int_{-\infty}^{\eta}[I_{-1/2}(\eta)]^2 d\eta}{I_{1/2}^{4/3}(\eta)}. \tag{19}$$

The corresponding expressions for the second-order gradient correction to the LDA exchange free-energy [13–16] (see also [22]) are

$$f_{\rm x}^{(2)}(n,\nabla n,{\rm T}) = e_{\rm x}^{\rm LDA}(n)\frac{8}{81}s^2\widetilde{B}_{\rm x}, \tag{20}$$

with

$$\widetilde{B}_{\rm x}(\eta) := \frac{3^{4/3}}{2^{4/3}}I_{1/2}^{4/3}(\eta)\left[\left(\frac{I'_{-1/2}(\eta)}{I_{-1/2}(\eta)}\right)^2 - 3\frac{I''_{-1/2}(\eta)}{I_{-1/2}(\eta)}\right]. \tag{21}$$

Primes denote derivatives with respect to the argument.

Practical implementation of all the combinations of FD integrals discussed above and implementation of density functionals with explicit T-dependence based on variables related to these combinations (for example, the T-dependent variables related to $\widetilde{B}$ in the GGA non-interacting free-energy [10]), require accurate analytical representations for the quantities in Eqs. (8) or (9), (12), (14)–(16), (19), and (21).

For ease of use of the results, Table 1 provides a cross-reference of all these quantities to both the analytical forms and the tables of coefficients provided in the fits we present here. Note that the quantity $\eta_{1/2}$ in the last line of Table 1 is the function inverse to $I_{1/2}(\eta)$. Detail about it is in Section 4.

3. Asymptotic behaviors as constraints

Knowledge of the asymptotic forms for the combinations just discussed is important for constraining analytical representations of them. Without such constraints, representations fitted over a finite independent-variable domain become uncontrolled approximations outside that domain. There are two relevant limits.

In the non-degenerate limit ($\eta \ll -1$), which corresponds to $y \to 0$, the functions given in Eqs. (8), (9), (12), (14)–(16), (19) and (21) have the following asymptotic expansions in terms of the variable y:

$$f(y) = -1 + \ln\left(\frac{2}{\sqrt{\pi}}y\right) + O(y),$$
$$\kappa(y) = \frac{5\times 2^{2/3}}{3^{5/3}}y^{-2/3}\left(-1+\ln\left(\frac{2}{\sqrt{\pi}}y\right)\right) + O(y^{1/3}),$$
$$\widetilde{B}(y) = 3 - \frac{3y}{\sqrt{2\pi}} + O(y^2),$$
$$\widetilde{C}(y) = \left(\frac{3}{2}\right)^{5/3}y^{2/3} + O(y^{5/3}),$$
$$\widetilde{D}(y) = \left(\frac{2}{3}\right)^{1/3}y^{2/3} + O(y^{5/3}),$$
$$\widetilde{E}(y) = \frac{3^{8/3}}{2^{25/6}}\frac{y^{5/3}}{\sqrt{\pi}} + O(y^{8/3}),$$
$$\widetilde{A}_{\rm x}(y) = \frac{2^{4/3}}{3^{4/3}}y^{2/3} + O(y^{5/3}),$$
$$\widetilde{B}_{\rm x}(y) = -\frac{3^{4/3}}{2^{1/3}}y^{4/3} + O(y^{7/3}). \tag{22}$$

Bearing in mind that $y = y(\eta)$, the foregoing relationships are derived as follows. The series expansion for $I_\alpha(\eta)$ ($\alpha > -1$, $\eta \le 0$) (see [23,24] for details) is

$$I_\alpha(\eta) = \Gamma(\alpha+1)e^\eta\sum_{k=0}^{\infty}(-1)^k\frac{e^{k\eta}}{(k+1)^{\alpha+1}}. \tag{23}$$

In the non-degenerate limit, the leading terms of Eq. (23) for $\alpha = 1/2$ are

$$y \equiv I_{1/2}(\eta) \approx \frac{\sqrt{\pi}}{2}e^\eta\left(1-\frac{e^\eta}{2\sqrt{2}}\right). \tag{24}$$

After series expansion of the negative solution to this quadratic in e^η, one has the inversion

$$\eta(y) = \ln\left(\frac{2}{\sqrt{\pi}}y\right) + \frac{y}{\sqrt{2\pi}} + O(y^2). \tag{25}$$

Next, consider the first two leading terms in the non-degenerate limit for FD integrals with indices $\alpha = 3/2, -1/2$ from Eq. (23). For those with indices $\alpha = -3/2, -5/2, -7/2$, and $-9/2$, we first use the recursion relation Eq. (2), then substitute the result from Eq. (24) to obtain

$$I_{3/2}(\eta) \approx \frac{3\sqrt{\pi}}{4}e^\eta\left(1-\frac{e^\eta}{4\sqrt{2}}\right),$$
$$I_{-1/2}(\eta) \approx \sqrt{\pi}e^\eta\left(1-\frac{e^\eta}{\sqrt{2}}\right),$$
$$I_{-3/2}(\eta) \approx -2\sqrt{\pi}e^\eta\left(1-\sqrt{2}e^\eta\right). \tag{26}$$

Remark. Eq. (23) also provides the leading terms correctly for $\eta \ll -1$ independent of α.

Elimination of the η variable in these leading terms via Eq. (25), substitution into equations for the quantities of interest, e.g. f, κ, $\widetilde{B}$, etc. defined by Eqs. (8)–(9), (12), (14)–(16), (19)–(21), and subsequent small-y series expansion up through the first y-dependent term (if necessary) yields Eqs. (22).

Remark. It is important to note that only the expansion for $\widetilde{B}$ requires use of the two leading terms in the FD series and subsequent small-y series expansion, but even in that specific case, the second term in Eq. (25) does not contribute to the final result, thus can be dropped in the process of elimination of the η variable. All the other expansions in Eq. (22) can be obtained with just the first term in Eqs. (24)–(26).

Conversely, in the degenerate limit $y \to \infty$ ($\eta \gg 1$), the leading terms in the asymptotic expansions of the FD integral combinations under consideration are

$$f(y) = \frac{3}{5}\left(\frac{3}{2}\right)^{2/3}y^{2/3} + O(y^{-2/3}),$$
$$\kappa(y) = 1 - \frac{5}{2^{2/3}3^{7/3}}\pi^2y^{-4/3} + O(y^{-8/3}),$$
$$\widetilde{B}(y) = 1 + \frac{2^{4/3}}{3^{7/3}}\pi^2y^{-4/3} + O(y^{-8/3}),$$

$$\widetilde{C}(y) = 1 + \frac{17}{2^{5/3}3^{7/3}}\pi^2 y^{-4/3} + O(y^{-8/3}),$$
$$\widetilde{D}(y) = 1 + \frac{413}{2^{2/3}3^{16/3}}\pi^2 y^{-4/3} + O(y^{-8/3}),$$
$$\widetilde{E}(y) = 1 + \frac{47}{2^{5/3}3^{7/3}}\pi^2 y^{-4/3} + O(y^{-8/3}),$$
$$\widetilde{A}_x(y) = 1 - \frac{2^{4/3}}{3^{10/3}}\pi^2 y^{-4/3}\Big(\ln(y) + const.\Big) + O(y^{-8/3}),$$
$$\widetilde{B}_x(y) = 1 + \frac{1}{2^{2/3}3^{1/3}}\pi^2 y^{-4/3} + O(y^{-8/3}). \quad (27)$$

The derivation of these expressions is essentially the same as for the opposite limit. The asymptotic series for $I_\alpha(\eta)$, now for $\eta > 0$, is (see Ref. [25, Eq. (3.10)], but note that they use the Dingle [26] normalization for the FD integrals)

$$I_\alpha(\eta) \sim \Gamma(\alpha+1)\left\{\cos(\alpha\pi)I_\alpha(-\eta) + \sum_{\nu=0}^{\infty}\frac{2\tau_{2\nu}}{\Gamma(\alpha+2-2\nu)}\eta^{\alpha+1-2\nu}\right\}$$
$$\tau_n := \sum_{m=1}^{\infty}\frac{(-1)^{m+1}}{m^n} = [1-2^{(1-n)}]\zeta(n) \quad (28)$$

with $\zeta(n)$ the Riemann zeta function. (Also see Ref. [26] and Eq. (5) in Ref. [27]). Thus, the equation analogous to Eq. (24) in the degenerate limit is

$$I_{1/2}(\eta) \approx \frac{2}{3}\eta^{3/2} + \frac{\pi^2}{12}\eta^{-1/2}. \quad (29)$$

The second term may be dropped, which gives the inversion

$$\eta(y) = \left(\frac{3}{2}\right)^{2/3} y^{2/3}. \quad (30)$$

Correspondingly, the leading terms in the degenerate limit of other relevant FD integrals are

$$I_{3/2}(\eta) \approx \frac{2}{5}\eta^{5/2} + \frac{\pi^2}{4}\eta^{1/2},$$
$$I_{-1/2}(\eta) \approx 2\eta^{1/2} - \frac{\pi^2}{12}\eta^{-3/2},$$
$$I_{-3/2}(\eta) \approx -2\eta^{-1/2} - \frac{\pi^2}{4}\eta^{-5/2}. \quad (31)$$

Again, elimination of the η variable in these leading terms, substitution into the equations for the quantities of interest, and one more series expansion (if needed) in the large-y limit up through the first y-dependent term yields the large-y asymptotic expressions of Eqs. (27).

Some of the results presented in Eqs. (22) and (27) can be found in Refs. [8,21]. Comparison between accurately evaluated reference data (see Section 5.2) and values obtained with terms in Eqs. (22) and (27) at extremely small-y and large-y also was used for verification of the expansion coefficients in Eqs. (22) and (27).

4. Inverse functions

We have already mentioned the importance of functions inverse to Fermi–Dirac integrals. These arise, for example, in problems related to the description of the electron gas at finite-T. Perhaps the most familiar example is the solution of Eq. (3) or, equivalently, of Eq. (6). Either requires the inverse to the function $I_{1/2}(\eta)$ to obtain the dimensionless Fermi energy $\eta = \beta\mu$. For the sake of generality, we define the inverse function for an FD integral of order α as

$$\eta_\alpha(I_\alpha(\eta)) := \eta. \quad (32)$$

The only one of interest here is

$$\eta_{1/2}(y) = \eta. \quad (33)$$

Various analytical fits (as a function of the y variable) to the solution of this specific inversion problem have been proposed [28,18]. The leading terms in the series expansion for $\eta_{1/2}$ in the non-degenerate and degenerate limits are given by Eqs. (25) and (30) respectively,

$$\eta_{1/2}(y) = \ln\left(\frac{2}{\sqrt{\pi}}y\right) + O(y); \quad y \to 0,$$
$$\eta_{1/2}(y) = \left(\frac{3}{2}\right)^{2/3} y^{2/3} + O(y^{-2/3}); \quad y \to \infty. \quad (34)$$

Analogous terms in the small-y and large-y expansions for other inverse functions $\eta_\alpha(y)$ could be obtained by inversion of Eqs. (26) and (31). We have not needed such inverse functions, so do not consider them here.

5. Smooth analytical representations

5.1. Context

In Ref. [8] Perrot provided analytical representations for both f and $\widetilde{B}$. Ref. [20] gave fits for $\widetilde{B}, \ldots, \widetilde{E}$. Both works used least squares fits (LSF) of Chebyshev polynomials to tabulations of calculated FD integrals. Such fits rely upon reference data on a finite interval of the variable $\eta \in [\eta_{\min}, \eta_{\max}]$. This is equivalent to mapping $y \in [y_{\min}, y_{\max}]$ onto the polynomial argument on the interval $[-1, 1]$. In Ref. [8], the data are tabulated on the interval $\eta \in [-10, 20]$. The corresponding y variable interval was divided into $[4 \cdot 10^{-5}, y_0]$ and $[y_0, 59.8]$, where $y_0 = 3\pi/4\sqrt{2}$. At y_0, the function and its first and second derivatives were required to be continuous. The advantage of using two intervals is that the small-y and large-y asymptotic behaviors can be incorporated easily in the fits, thereby making them applicable for the entire range $y \in [0, \infty[$. The disadvantage is that the fits turn out not to be smooth near y_0 despite the enforcement of continuity. Numerical illustrations of the issue in the case of the fit to $\widetilde{B}$ from Ref. [8] are provided in the next sub-Section. Note that the fit to f is smooth through the second derivative.

For the second- and fourth-order gradient corrections to the non-interacting free energy, Geldart and Sommer [20] also used Chebyshev polynomials, but fitted to tabulated data on the entire interval $y \in [0.02, 25]$. They thereby avoided the problem of connection at an intermediate point. The drawback is that there is no straightforward means to incorporate the asymptotic behaviors beyond the ends of the interval.

Ref. [29] provided a fit to the LDA exchange Eq. (17) in the form of a Padé approximant of order [4,4] in terms of the variable t. The accuracy of that fit is examined below.

A simple fit to the inverse $\eta_{1/2}$ function is given by Eq. (8) of Ref. [28] (see also Eq. (38) in Ref. [18] and Table 2 for the fit accuracy). Ref. [30] provides a rational function approximation for inverse functions of selected FD integrals. Though those fits are accurate, the approximations again are on two separate domains of the corresponding independent variable. That immediately brings into play the possibility of continuity problems with functional derivatives. Also, the most accurate approximation provided in Ref. [30] has a significantly larger number of parameters than the analytical representation given in the next subsection.

Table 2
Results for present work ("PADE") using LSF and combined MARE fitting (see text) compared with fits from Perrot [8], Geldart and Sommer (GS) [21], Perrot–Dharma-wardana (PDW84) [29], and Nilsson Eq. (8) in Ref. [28] (same as Blakemore Eq. (38) in Ref. [18]). Relative square error (RSE) (in %) for the specified fitted function is in column two. Mean absolute relative error (MARE) (in %) for that fitted function (F) and for its first (F') and second (F'') derivatives with respect to the variable y are in the third, fourth, and fifth columns.

Fit	RSE(F)	MARE(F)	MARE(F')	MARE(F'')
$\kappa(y)$				
Perrot	$7.0 \cdot 10^{-10}$	0.0002	0.004	0.013
$\widetilde{B}(y)$				
Perrot	$2.4 \cdot 10^{-6}$	0.008	1.5	2.1
GS[a]	$5.4 \cdot 10^{-4}$	0.23	37	581
Padé (LSF)	$1.0 \cdot 10^{-8}$	0.001	0.52	0.72
Padé (MARE fit)	$4.5 \cdot 10^{-8}$	0.0004	0.017	0.055
$\widetilde{C}(y)$				
GS[a]	$1.5 \cdot 10^{-3}$	0.63	21	736
Padé (LSF)	$2.3 \cdot 10^{-7}$	0.01	0.65	0.73
Padé (MARE fit)	$2.5 \cdot 10^{-6}$	0.008	0.17	0.31
$\widetilde{D}(y)$				
GS[a]	$1.2 \cdot 10^{-3}$	0.80	10	135
Padé (LSF)	$8.8 \cdot 10^{-7}$	0.013	1.1	1.3
Padé (MARE fit)	$3.3 \cdot 10^{-5}$	0.015	0.47	0.67
$\widetilde{E}(y)$				
GS[a]	$1.9 \cdot 10^{-3}$	10	6.7	47
Padé (LSF)	$1.7 \cdot 10^{-6}$	0.037	1.1	1.4
Padé (MARE fit)	$2.5 \cdot 10^{-5}$	0.027	0.50	0.93
$\widetilde{A}_x(y)$				
PDW84	$5.9 \cdot 10^{-2}$	0.19	27	23
Padé (LSF)	$3.3 \cdot 10^{-9}$	0.001	0.05	0.07
Padé (MARE fit)	$1.7 \cdot 10^{-8}$	0.001	0.02	0.04
$\widetilde{B}_x(y)$				
Padé (LSF)	$1.3 \cdot 10^{-6}$	0.021	0.67	1.4
Padé (MARE fit)	$1.0 \cdot 10^{-5}$	0.023	0.32	0.49
$\eta_{1/2}(y)$				
Nilsson	0.7	8.5	6.9	6.6
Padé (LSF)	$1.3 \cdot 10^{-10}$	0.0015	0.0028	0.040
Padé (MARE fit)	$4.0 \cdot 10^{-10}$	0.0009	0.0026	0.035

[a] Fit from Ref. [21]; errors calculated only on the interval $y \in [0.02, 25]$ used for fitting.

5.2. Present work—analytical representations and fitting

In contrast with prior practice, we used both a standard LSF and augmented non-linear fits (discussed below) to data we calculated on a large interval, $\eta \in [-11, 100]$. That corresponds to $y \in [1.48 \cdot 10^{-5}, 667]$ and $t \in [0.01, 1266]$. The tabulation was on a uniform η mesh with increment $\Delta\eta = 0.025$. Excluding two boundary points from each end gives a total of $N = 4436$ mesh points. FD integrals of order $\alpha = 3/2, 1/2, -1/2$ and their first and second derivatives were calculated by the quadrature methodology presented in Ref. [31]. The version that uses 80 evaluations of the integrand and guarantees about 15 decimal digits accuracy was employed.

For $\alpha = -3/2, -5/2, -7/2$, and $-9/2$, the FD integrals were calculated using the recursion relation Eq. (2) with commuted differentiation and integration,

$$I_{\alpha-k}(\eta) = \frac{\Gamma(\alpha)}{\Gamma(\alpha-k+2)} \int_0^\infty dx \left(\frac{d}{d\eta}\right)^k \frac{x^\alpha}{1+\exp(x-\eta)} \tag{35}$$

with $\alpha = -1/2$ and $k = 1, 2, 3, 4$. The derivatives were done analytically and the integration by the same quadrature method as for the other indices.

The FD integral in the numerator of $\widetilde{A}_x(\eta)$, Eq. (19), was separated into two parts,

$$\widetilde{A}_x(\eta) = \frac{2^{1/3}}{3^{4/3}} \left[\frac{\int_{-\infty}^{\eta_1} [I_{-1/2}(\eta)]^2 d\eta + \int_{\eta_1}^{\eta} [I_{-1/2}(\eta)]^2 d\eta}{I_{1/2}^{4/3}(\eta)} \right], \tag{36}$$

where η_1 is the first mesh point ($\eta_1 = -11$ which corresponds to $y_1 \equiv y(\eta_1) = 1.48 \cdot 10^{-5}$). The first integral in this expression was calculated using the small-y series expansion for $\widetilde{A}_x$ (see Eq. (22)), $\int_{-\infty}^{\eta_1} [I_{-1/2}(\eta)]^2 d\eta = 3^{4/3} 2^{-1/3} \widetilde{A}_x(y(\eta_1)) I_{1/2}^{4/3}(\eta_1)$. The second term was evaluated numerically on the uniform η mesh described above using Simpson's rule with additional evaluation of the integrand at intermediate points $\eta_i + \Delta\eta/2$. Derivatives of all FD integral combinations with respect to the variable y were done numerically.

Regarding the analytical forms to represent the FD integral combinations of interest, greater flexibility is required than is provided by Chebyshev polynomials if the leading asymptotic terms for both small- and large-y limits are to be incorporated. Moreover, the resulting representations should be intrinsically continuous (including all derivatives) on the entire range of $y \in [0, \infty[$. These considerations led to the adoption of Padé approximants [17] for the basic representations. As will become apparent, augmentation is required in some cases. The method can be sketched as follows: (i) select appropriate variables for two polynomials in the form $y^{m/3}$, where $m = 1, 2, 3$ or 4; (ii) constrain appropriate coefficients to match small-y and large-y series expansions; (iii) fit the remaining coefficients.

Because the fits to κ, $\widetilde{A}_x$ and $\eta_{1/2}$ require use of modified approximants which incorporate logarithmic terms, it is simplest to begin with $\widetilde{B}$. The leading terms of its asymptotic expansions, Eqs. (22) and (27), dictate the choice of fitting function to be

$$\widetilde{B}(y) = \frac{\sum_{i=0}^{8} a_i y^i}{1 + \sum_{i=1}^{12} b_i u^i}, \tag{37}$$

where $u = y^{2/3}$. This is a Padé approximant of order [24, 24] with respect to the variable $y^{1/3}$. Correct powers of the first few terms in the small-y and large-y asymptotic expansions are assured by setting $a_7 = b_1 = b_2 = b_4 = b_{11} = 0$. Doing so eliminates terms in $y^{2/3}$, $y^{4/3}$, $y^{5/3}$, $y^{7/3}$, $y^{8/3}$, and in $y^{-2/3}$, y^{-1}, $y^{-5/3}$, $y^{-7/3}$ from the small- and large-y asymptotic expansions respectively. Agreement with the correct coefficients for the leading small-y expansion terms requires $a_0 = 3$ and $a_1 = -3/\sqrt{2\pi}$. Similarly, the large-y asymptotic expansion coefficients are matched by setting $b_{12} = a_8$ and $b_{10} = -2^{4/3}3^{-7/3}\pi^2 b_{12}$. The remaining coefficients could, in principle, be set by LSF but that turns out not to be best. See discussion below.

Turning next to $\widetilde{C}$, $\widetilde{D}$, and $\widetilde{E}$, because their small-y expansions have terms proportional to powers of $y^{1/3}$ (see Eqs. (22) and (27)), the fitting functions are of the form

$$R(y) = \frac{a_{2.5}u^{5/2} + \sum_{i=1}^{12} a_i u^i}{1 + \sum_{i=1}^{6} b_i v^i}, \tag{38}$$

where $v = y^{4/3}$. The term $\propto u^{5/2}$ is added to match the $y^{5/3}$ term present in the small-y expansion. Eq. (38) has the form of a [24,24] Padé approximant with respect to the variable $y^{1/3}$. Setting $a_{11} = 0$ in Eq. (38) for $\widetilde{C}$ and $\widetilde{D}$ eliminates the $y^{-2/3}$ term in the large-y asymptotic expansion. We found it beneficial to keep terms in $y^{4/3}$ and y^{-2} in the small-y and large-y expansions correspondingly, in that doing so reduces fitting errors considerably. Setting $a_1 = a_2 = a_{11} = 0$ for $\widetilde{E}$ eliminates terms proportional to $y^{2/3}$ and $y^{-2/3}$ in the asymptotic expansions. Again, keeping y^2 and y^{-2} terms in the small- and large-y expansions led to reduced fitting errors. Additional constraints on the parameters in Eq. (38) arise from fixing the coefficients of the leading terms in small-y and large-y expansions Eqs. (22) and (27) (see corresponding Tables in the Appendix).

Fitting of $\widetilde{A}_x(y)$ requires incorporation of a logarithmic term to satisfy the large-y asymptotic expansion (see Eq. (27)). The modified Padé approximant of order [16,16] (with respect to the variable $y^{1/3}$) is similar to Eq. (38) (with the additional log term in the numerator),

$$\widetilde{A}_x(y) = \frac{a_{ln}y^4 \ln(y) + a_{2.5}u^{5/2} + \sum_{i=1}^{8} a_i u^i}{1 + \sum_{i=1}^{4} b_i v^i}. \tag{39}$$

Setting $a_7 = 0$ in Eq. (39) eliminates the un-needed $y^{-2/3}$ dependence in the large-y expansion. See Table 7 for additional constraints on the parameters.

Similarly, fitting of either the function f or κ requires incorporation of logarithmic terms in a modified Padé approximant. We developed such a modified Padé approximant as well (not shown here), but fitting to it did not yield any material improvement with respect to the original Perrot fit [8] which has very small relative errors (see Table 2).

The representation of $\widetilde{B}_x$ takes the form of a [20, 20] Padé approximant

$$\widetilde{B}_x(y) = \frac{\sum_{i=2}^{10} a_i u^i}{1 + \sum_{i=1}^{10} b_i u^i}, \tag{40}$$

where $a_1 = a_9 = b_9 = 0$ to eliminate the $y^{2/3}$ and $y^{-2/3}$ terms from the small-y and large-y expansions respectively. Additional constraints are imposed on the parameters a_2, b_8 and b_{10} to match the coefficients of the leading terms in Eqs. (22) and (27) (see Table 8).

The fitting function for $\eta_{1/2}$ is similar to that of Eq. (39) due to the presence of the logarithmic term in the asymptotic expansion. Also, the constant a_0 and the ninth power of the variable u were added in the numerator to satisfy the large-y expansion Eq. (34), that is,

$$\eta_{1/2}(y) = \frac{a_{ln}\ln(y) + a_{2.5}u^{5/2} + \sum_{i=0}^{9} a_i u^i}{1 + \sum_{i=1}^{4} b_i v^i}. \tag{41}$$

We take $a_8 = 0$ to eliminate a constant term in the large-y expansion (see Eq. (34)) and $a_0 = \ln(2/\sqrt{\pi})$, $a_{ln} = 1$, $b_4 = (2/3)^{2/3}a_9$ to match the expansion coefficients in Eq. (34). Again, we found it beneficial to keep the $u^{5/2}$ term to reduce fitting errors.

Eventually, the fit to $\widetilde{B}$ has 12 independent parameters, while the $\widetilde{C}$, $\widetilde{D}$, $\widetilde{E}$ fits have 15 and the fits to $\widetilde{A}_x$ and $\widetilde{B}_x$ have 10 and 14 parameters, respectively. The fitted inverse function $\eta_{1/2}$ has 12 independent parameters. For comparison, the Perrot fits [8] have 15 and 14 parameters for κ and $\widetilde{B}$ respectively. The fits to $\widetilde{B}$–$\widetilde{E}$ from Ref. [21] have, in order, 10, 20, 9, and 14 parameters. All parameters, including constrained ones, are listed in Tables 3–9.

The remaining issue is determination of the coefficients left undetermined after enforcement of the asymptotic criteria. Numerical exploration led to the conclusion that ordinary LSF techniques are not adequate for that task. The standard LSF criterion is to minimize the squared error (SE) $\mathcal{E}_{SE} := \sum_{i=1}^{N}(F_i - F_{fit,i})^2$, which is related to the relative squared error (RSE)

$$\mathcal{E}_{RSE} := \frac{\sum_{i=1}^{N}(F_i - F_{fit,i})^2}{\sum_{i=1}^{N} F_i^2}. \tag{42}$$

However, a small SE (or a small RSE) obviously does not guarantee a small mean absolute relative error (MARE) for a function and the derivatives of that fitted function. Both a more sensitive measure and one which takes explicit account of at least the low-order derivatives are required. Hence we adopted fitting based on a weighted MARE criterion. With the MARE for a function F defined as

$$\mathcal{E}_{MARE}[F] := N^{-1}\sum_{i=1}^{N}\frac{|F_i - F_{fit,i}|}{|F_i|}, \tag{43}$$

the weighted error we minimized was

$$\omega[F] = 10 \times \mathcal{E}_{MARE}[F] + \mathcal{E}_{MARE}[F'(y)] + \mathcal{E}_{MARE}[F''(y)]. \tag{44}$$

Here F is considered as a function of the variable y and primes once again indicate the derivatives. The ratio of 10:1:1 for relative weights was chosen with the intent of emphasizing the accuracy of the analytical representations of the functions themselves, with reduction of the MARE for the derivatives as secondary criteria. However the results do not depend sensitively on the relative weight of the function MARE with respect to the derivative MAREs. The RSE and MARE results also depend rather weakly on the choice of the $\Delta\eta$ for spacing the reference data and on the size of the η interval (see previous sub-Section for the choice used here).

5.3. Accuracy

Table 2 shows the RSE for fitted functions and MARE for the functions and their first and second derivatives for the current work with pure LSF and with the weighted MARE optimization

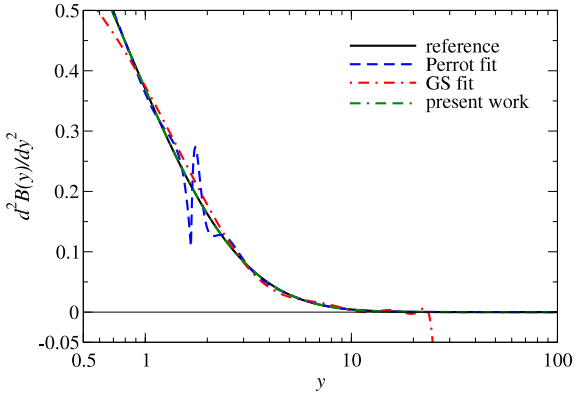

Fig. 1. Second derivative $\widetilde{B}''(y)$ as a function of y. Comparison between reference data and Perrot, GS, and weighted MARE Padé fits.

from Eq. (44). These are compared with the previous representations from Perrot [8] and Geldart and Sommer [21] fits. Perrot's fit for $\kappa(y)$ yields very small MARE values for both the function and its first and second derivatives, i.e., the fit provides an accurate analytical representation for κ (or, equivalently f). Perrot's fit to $\widetilde{B}(y)$ yields a small MARE for the function, but the MAREs for the first and second derivatives are not small (1.5% and 2.1% correspondingly). The Geldart and Sommer fits provide acceptable MAREs for the representations of $\widetilde{B}$, $\widetilde{C}$, and $\widetilde{D}$, but not for $\widetilde{E}$, for which the MARE is 10%. However, the GS fits fail completely for the derivatives, with MARE values from 6.7% up to 736%.

Our Padé (and modified Padé) fits based on the weighted MARE criterion provide generally superior results. MARE values for fitted functions are between 0.0004% and 0.027%. MAREs for derivatives of $\widetilde{B}$ and $\widetilde{A}_x$ are of the order of hundredths of percent. For the derivatives of $\widetilde{C}$, $\widetilde{D}$, $\widetilde{E}$ and $\widetilde{B}_x$ the MAREs are less than one percent.

Unsurprisingly, the second derivative is the most sensitive quantity to fitting errors. Fig. 1 shows the second derivative $\widetilde{B}''(y)$ calculated from the Perrot, GS, and our weighted MARE Padé fit compared to the reference calculated values. Overall, the Perrot fit provides good agreement with the tabulated data except in the region near $y_0 \approx 1.67$, where the second derivative has huge oscillations. The GS fit oscillates about the reference values over the entire range of y. In contrast, the weighted MARE Padé fit is smooth and generally in excellent agreement with the tabulated data. Mean absolute relative errors for the second derivative $\widetilde{B}''(y)$ are 2.1%, 580% and 0.055% for the Perrot, GS, and weighted MARE Padé fits correspondingly. Fig. 2 shows similar behavior from the GS fit for the second derivatives $\widetilde{C}''(y)$, $\widetilde{D}''(y)$ and $\widetilde{E}''(y)$. Comparison between the calculated reference data and the weighted MARE Padé fit for $\widetilde{B}''_x(y)$ is excellent (see Fig. 2) with an MARE of 0.55%.

In a similar vein, Fig. 3 compares reference data, the Perrot–Dharma-wardana (PDW84) [29], and modified Padé fits for $\widetilde{A}_x$ and its derivatives with respect to y. The maximum relative error of the PDW84 fit to $\widetilde{A}_x$ is about 0.7% (upper-left panel) at $y \approx 20$ ($t \approx 0.1$). That seemingly small error might be not negligible for certain calculations. As an example consider use of a fit to $\widetilde{A}_x$ for calculation of the LDA correlation free-energy per particle (f_c^{LDA}/n) from the LDA exchange–correlation free-energy, $f_c^{LDA}/n \equiv (f_{xc}^{LDA} - f_x^{LDA})/n$. At $t = 0.125$ ($y = 15.085$), $r_s = 1.0$ the PDW84 fit gives $f_c^{LDA}/n = -0.5200 + 0.4309 = -0.0891$ Hartree (see Table S1 in Supplemental Material for Ref. [11]). The accurate modified Padé fit introduced here gives $f_c^{LDA}/n = -0.5200 + 0.4278 = -0.0922$ Hartree, that is, about 3% lower. Moreover, despite the reasonably accurate fit provided by the PDW84 form (MARE = 0.19%), it does not provide accurate first and second derivatives. Fig. 3 also shows relative differences between reference data and corresponding fits for those derivatives. Errors in the first derivative of $\widetilde{A}_x(y)$ propagate as errors in the corresponding exchange potential

$$v_x^{LDA}(n,t) = \frac{\partial e_x^{LDA}(n)}{\partial n}\widetilde{A}_x(y(t)) + e_x^{LDA}(n)\frac{\partial \widetilde{A}_x(y(t))}{\partial t}\frac{\partial t}{\partial n}. \qquad (45)$$

Consequences of this error propagation are shown in the lower-right panel of Fig. 3, which compares exchange potentials from the present fit and the PDW84 fit with reference data, all calculated

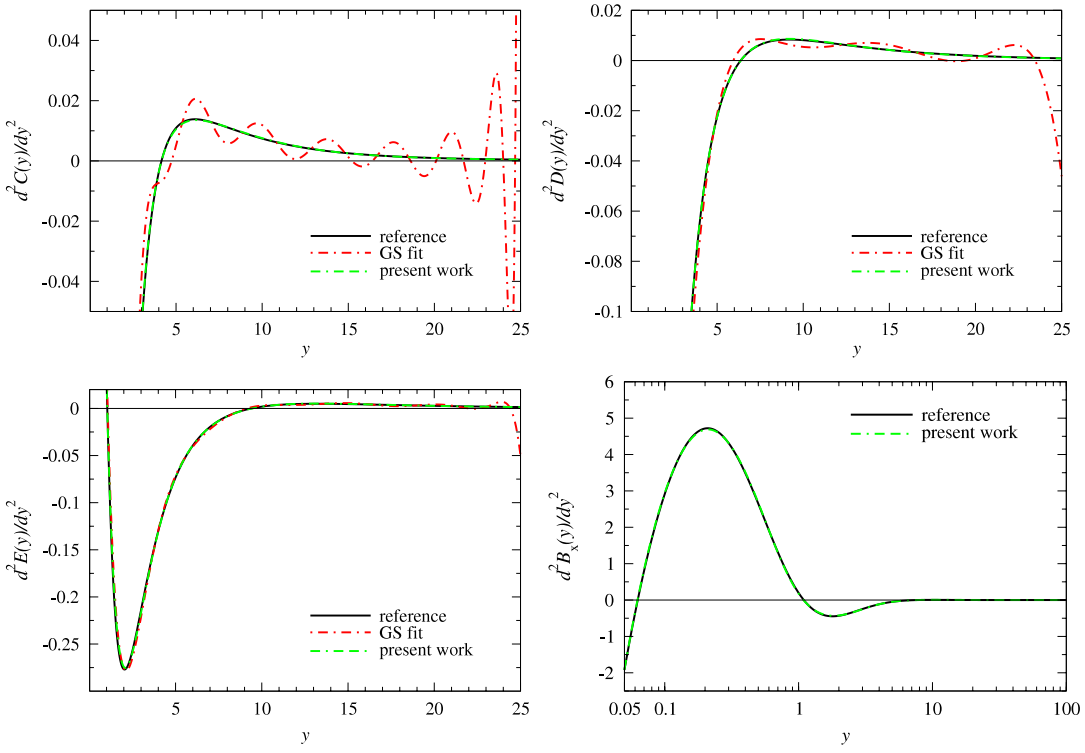

Fig. 2. Second derivatives $\widetilde{C}''(y)$, $\widetilde{D}''(y)$, $\widetilde{E}''(y)$ and $\widetilde{B}''_x(y)$ as functions of y. Comparison between reference data and fits.

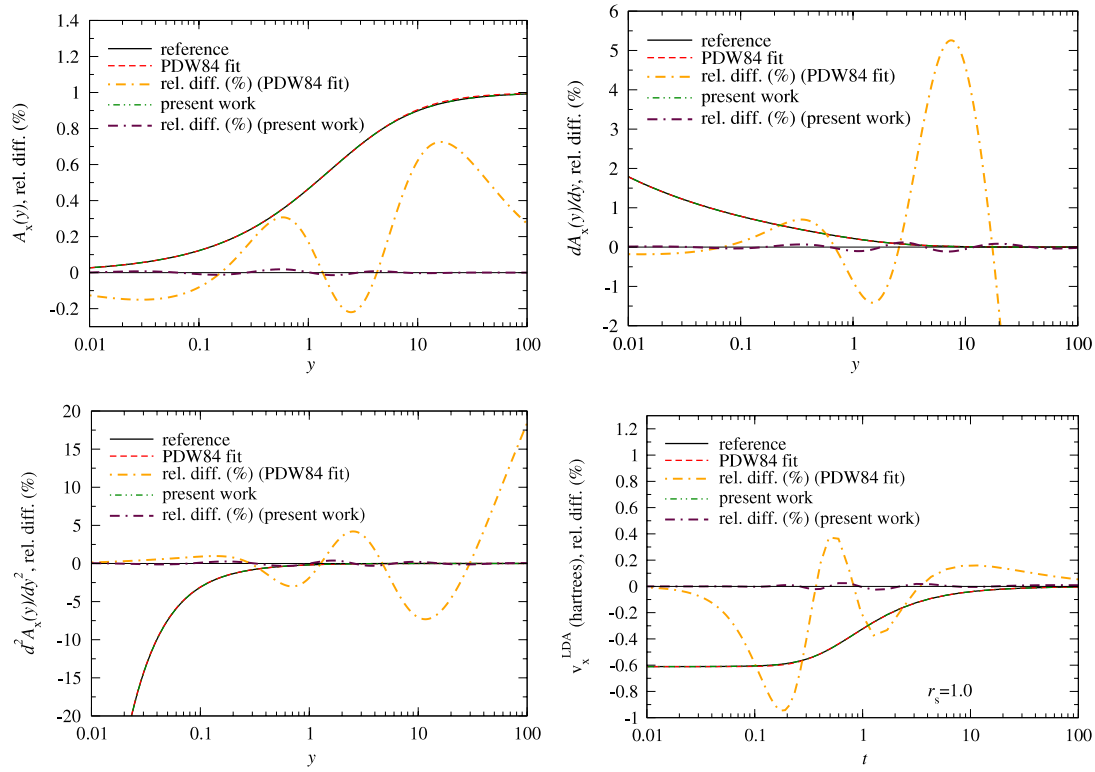

Fig. 3. Comparison between reference data and fits for $\widetilde{A}_x(y)$, $\widetilde{A}'_x(y)$ and $\widetilde{A}''_x(y)$ as functions of y. Relative differences between corresponding fits and reference data also are shown. The lower-right panel shows corresponding X potentials (as functions of t) and relative differences between reference v_x^{LDA} and values calculated from fits for $r_s = 1.0$ bohr.

for $r_s = (3/4\pi n)^{1/3} = 1$ bohr. The relative errors for v_x^{LDA} from the PDW84 fit are near 1% for $0.1 < t < 2$. Errors in v_x^{LDA} are reduced as compared to corresponding errors in the first derivative of $\widetilde{A}_x$ because the X potential is dominated by the first term in Eq. (45). Results for other values of r_s are similar. The fit based on the modified Padé approximant Eq. (39) provides practically perfect agreement with the reference data for $\widetilde{A}_x$, its first two derivatives, and for the corresponding exchange potential.

The last three lines of Table 2 show errors for fits to the inverse function $\eta_{1/2}$. The Nilsson fit [28,18] proves to be only a semi-quantitative approximation at best, with MAREs close to 10% for both the function and its derivatives. Our modified Padé MARE fit provides very accurate results, with MARE for the function only 0.0009%. The LSF provides practically the same accuracy.

6. Conclusions

We have developed accurate analytical representations for six combinations of Fermi–Dirac integrals and for one of the most important inverse functions arising in finite-T DFT. The representations have either the form of Padé approximants or modified Padé approximants as needed to accommodate required asymptotic behaviors. Parameters in the analytical forms are constrained to reproduce correctly the leading terms in the asymptotic expansions for both extremes of the variable y.

The new representations enable fast, accurate evaluation of the required FD integral combinations and their derivatives with improved accuracy compared to previously published fits. MAREs for the new representations are of the order of hundredths of a percent in worse cases. The new representations furthermore are intrinsically continuous with continuous derivatives of any order. The only previously published fit which has suitably small errors for both the function and its derivatives is that by Perrot for $f = 3\kappa/(5t)$. A set of FORTRAN subroutines for all the new improved fits and corresponding derivatives is available by download from http://www.qtp.ufl.edu/ofdft and by request to the authors.

Acknowledgments

We thank J.W. Dufty for helpful comments. We thank the University of Florida High-Performance Computing Center for computational resources and technical support. This work was supported by the US Dept. of Energy TMS grant DE-SC0002139.

Appendix

The coefficients of the Padé fits to $\widetilde{B}$, $\widetilde{C}$, $\widetilde{D}$, $\widetilde{E}$, $\widetilde{A}_x$, $\widetilde{B}_x$ and $\eta_{1/2}$ as functions of the y variable (see Eqs. (37)–(41)) are given in Tables 3–9. The second column shows the constraints imposed on corresponding coefficients. A "yes" signifies that the coefficient was constrained to be 0, 1, or 3 as the case may be.

Table 3
Coefficients in fit to $\widetilde{B}(y)$.

Coefficient	Constraint	Value
a_0	yes	3.0000000000000000
a_1	$-3/\sqrt{2\pi}$	−1.1968268412042982
a_2		427.3949714847699966
a_3		−170.1211444343163919
a_4		31.7020753506680002
a_5		3.3713851108273998
a_6		2.2529104734200001
a_7	yes	0.0000000000000000

(continued on next page)

Table 3 (*continued*)

Coefficient	Constraint	Value
a_8		0.0202417083225910
b_1	yes	0.0000000000000000
b_2	yes	0.0000000000000000
b_3		142.2807110810987865
b_4	yes	0.0000000000000000
b_5		0.5924932349226000
b_6		−18.0196644249469990
b_7		7.2322601129560002
b_8		0.1910870984626600
b_9		2.2522978973395000
b_{10}	$-2^{4/3}3^{-7/3}\pi^2 b_{12}$	−0.0387826345397392
b_{11}	yes	0.0000000000000000
b_{12}	a_8	0.0202417083225910

Table 4
Coefficients in fit to $\widetilde{C}(y)$.

Coefficient	Constraint	Value
$a_{2.5}$		5.9265262369781002
a_1	$3^{5/3}2^{-5/3}$	1.9655560456566725
a_2		−0.5768378962095700
a_3		35.9130119576930014
a_4		41.1168867899709980
a_5		−40.3677476700629967
a_6		59.6804384544149968
a_7		−0.3211461169282900
a_8		4.2815226867198000
a_9		0.0030385200207883
a_{10}		0.1596522984577500
a_{11}	yes	0.0000000000000000
a_{12}		0.0056843727998872
b_1		26.5710993646139997
b_2		20.1172145257690005
b_3		17.6858602829550016
b_4		3.6467884940180002
b_5	$(a_{10} - C \times b_6) \times b_6/a_{12}$[a]	0.1365086602125932
b_6	a_{12}	0.0056843727998872

[a] $C = 17 \times 2^{-5/3}3^{-7/3}\pi^2$.

Table 5
Coefficients in fit to $\widetilde{D}(y)$.

Coefficient	Constraint	Value
$a_{2.5}$		0.4524584047298800
a_1	$2^{1/3}3^{-1/3}$	0.8735804647362989
a_2		0.0300776040166210
a_3		14.3828916532949993
a_4		1.8670041583370001
a_5		37.9149736744980004
a_6		0.7589550686574100
a_7		16.9530731446740006
a_8		3.1373656916102002
a_9		0.0241382844920020
a_{10}		0.1538471708464500
a_{11}	yes	0.0000000000000000
a_{12}		0.0049093483855146
b_1		15.9188442750290005
b_2		29.1916070884210015
b_3		14.7377409947669999
b_4		3.1005334835656000
b_5	$(a_{10} - C \times b_6) \times b_6/a_{12}$[a]	0.1178771827774314
b_6	a_{12}	0.0049093483855146

[a] $C = 413 \times 2^{-2/3}3^{-16/3}\pi^2$.

Table 6
Coefficients in fit to $\widetilde{E}(y)$.

Coefficient	Constraint	Value
$a_{2.5}$	$3^{8/3}2^{-25/6}\pi^{-1/2}$	0.5881075583333214
a_1	yes	0.0000000000000000
a_2	yes	0.0000000000000000
a_3		−0.0132237512072000
a_4		0.5865252375234600
a_5		1.1120705517211000
a_6		2.2626091489173001
a_7		2.6723837550020000
a_8		0.3385116347002500
a_9		0.0038743130529412
a_{10}		0.0108166294882730
a_{11}	yes	0.0000000000000000
a_{12}		0.0003699371553596
b_1		2.8191769574094998
b_2		7.4555425143053000
b_3		2.5142144377484001
b_4		0.3944764252937600
b_5	$(a_{10} - C \times b_6) \times b_6/a_{12}$[a]	0.0066524832876068
b_6	a_{12}	0.0003699371553596

[a] $C = 47 \times 2^{-5/3}3^{-7/3}\pi^2$.

Table 7
Coefficients in fit to $\widetilde{A}_x(y)$.

Coefficient	Constraint	Value
a_{ln}	$C \times b_4$[a]	−0.0475410604245741
$a_{2.5}$		−0.1065378473507800
a_1	$2^{4/3}3^{-4/3}$	0.5823869764908659
a_2		−0.0068339509356661
a_3		11.5469239288490009
a_4		−0.8465428870889800
a_5		−0.1212525366470300
a_6		1.9902818786101000
a_7	yes	0.0000000000000000
a_8		0.0744389046707120
b_1		19.9256144707979992
b_2		5.1663994545590004
b_3		2.0463164858237000
b_4	a_8	0.0744389046707120

[a] $C = -2^{4/3}3^{-10/3}\pi^2$.

Table 8
Coefficients in fit to $\widetilde{B}_x(y)$.

Coefficient	Constraint	Value
a_2	$-3^{4/3}2^{-1/3}\pi^{-1/2}$	−3.4341427276599950
a_3		−0.9066069544311700
a_4		2.2386316137237001
a_5		2.4232553178542000
a_6		−0.1339278564306200
a_7		0.4392739633708200
a_8		−0.0497109675177910
a_9	yes	0.0000000000000000
a_{10}		0.0028609701106953
b_1		0.7098198258073800
b_2		4.6311326377185997
b_3		−2.9243190977647000
b_4		6.1688157841895004
b_5		−1.3435764191535999
b_6		0.1576046383295400
b_7		0.4365792821186800
b_8	$(a_8 - C \times b_{10}) \times b_{10}/a_{10}$[a]	−0.0620444574606262
b_9	yes	0.0000000000000000
b_{10}	a_{10}	0.0028609701106953

[a] $C = 2^{-2/3}3^{-1/3}\pi^2$.

Table 9
Coefficients in fit to $\eta_{1/2}(y)$.

Coefficient	Constraint	Value
a_{ln}	yes	1.0000000000000000
$a_{2.5}$		−1.2582793945794000
a_0	$\ln(2/\sqrt{\pi})$	0.1207822376352453
a_1		0.0233056178489510
a_2		1.0911595094936000
a_3		−0.2993063964300200
a_4		−0.0028618659615192
a_5		0.5051953653801600
a_6		0.0419579806591870
a_7		1.3695261714367000
a_8	yes	0.0000000000000000
a_9		0.2685157355131100
b_1		0.0813113962506270
b_2		1.1903358203098999
b_3		1.1445576113258000
b_4	$(2/3)^{2/3}a_9$	0.2049158578610270

References

[1] N.D. Mermin, Phys. Rev. 137 (1965) A1441.
[2] M.V. Stoitsov, I. Zh. Petkov, Ann. Physics 185 (1988) 121.
[3] R.M. Dreizler, in: W. Greiner, H. Stöcker (Eds.), The Nuclear Equation of State, Part A, NATO ASI, vol. B216, Plenum, NY, 1989, p. 521.
[4] M.P. Desjarlais, J.D. Kress, L.A. Collins, Phys. Rev. E 66 (2002) 025401.
[5] D.A. Horner, F. Lambert, J.D. Kress, L.A. Collins, Phys. Rev. B 80 (2009) 024305.
[6] V.V. Karasiev, D. Chakraborty, O.A. Shukruto, S.B. Trickey, Phys. Rev. B 88 (2013) 161108(R).
[7] R.P. Feynman, N. Metropolis, E. Teller, Phys. Rev. 75 (1949) 1561.
[8] F. Perrot, Phys. Rev. A 20 (1979) 586.
[9] J. Bartel, M. Brack, M. Durand, Nuclear Phys. A 445 (1985) 263.
[10] V.V. Karasiev, T. Sjostrom, S.B. Trickey, Phys. Rev. B 86 (2012) 115101.
[11] V.V. Karasiev, T. Sjostrom, J. Dufty, S.B. Trickey, Phys. Rev. Lett. 112 (2014) 076403.
[12] B. Horovitz, R. Thieberger, Physica 71 (1974) 99.
[13] E. Dunlap, D.J.W. Geldart, Can. J. Phys. 72 (1994) 1.
[14] M.L. Glasser, D.J.W. Geldart, E. Dunlap, Can. J. Phys. 72 (1994) 7.
[15] E. Dunlap, D.J.W. Geldart, Can. J. Phys. 72 (1994) 14.
[16] D.J.W. Geldart, E. Dunlap, M.L. Glasser, M.R.A. Shegelski, Solid State Commun. 88 (1994) 81.
[17] G.A. Baker, J.L. Gammel (Eds.), The Pade Approximant in Theoretical Physics, Academic Press, NY, 1970.
[18] J.S. Blakemore, Solid-State Electron. 25 (1982) 1067.
[19] K. Huang, Statistical Mechanics, J. Wiley and Sons, NY, 1963, p. 224. Eq. (11.2).
[20] D.J.W. Geldart, E. Sommer, Phys. Lett. 108A (1985) 103.
[21] D.J.W. Geldart, E. Sommer, Phys. Rev. B 32 (1985) 7694.
[22] D.J.W. Geldart, Top. Curr. Chem. 180 (1996) 31.
[23] J.P. Cox, R.T. Giuli (Eds.), Principles of Stellar Structure, Gordon & Breach, New York, 1968.
[24] L.D. Cloutman, Astrophys. J. Suppl. Ser. 71 (1989) 677.
[25] T.M. Garoni, N.E. Frankel, M.L. Glasser, J. Math. Phys. 42 (2001) 1860.
[26] R.B. Dingle, Appl. Sci. Res. Ser. B 6 (1957) 225.
[27] W.J. Cody, H.C. Thacher Jr., Math. Comp. 21 (1967) 30;
W.J. Cody, H.C. Thacher Jr., Math. Comp. 21 (1967) 525. Corrigiendum.
[28] N.G. Nilsson, Phys. Status Solidi (a) 19 (1973) K75.
[29] F. Perrot, M.W.C. Dharma-wardana, Phys. Rev. A 30 (1984) 2619.
[30] H.M. Antia, Astrophys. J. Suppl. 84 (1993) 101.
[31] J.M. Aparacio, Astrophys. J. Suppl. Ser. 117 (1998) 627.